DEPARTMENT OF CIVIL ENGINEERING AND ENGINEERING MECHANICS

COLUMBIA UNIVERSITY

Response of Space Shuttle Insulation Panels to Acoustic Noise Pressure

by

R. Vaicaitis

June 1976
Technical Report No. 2

Prepared for the National Aeronautics and Space Administration
Under Grant No. NSG-1059

DEPARTMENT OF CIVIL ENGINEERING AND ENGINEERING MECHANICS

COLUMBIA UNIVERSITY

Response of Space Shuttle Insulation Panels to Acoustic Noise Pressure

by

R. Vaicaitis

June 1976
Technical Report No. 2

Prepared for the National Aeronautics and Space Administration
Under Grant No. NSG-1059

1. Introduction

In the present paper the response of reusable space shuttle surface insulation panels to convecting random pressure field are studied. The current design concept for the Thermal Protection System (TPS) heat shield panels of the space shuttle consist of a relatively thick ceramic tile mounted on a soft (viscoelastic) foundation, a so-called "strain-isolator", which in turn is bonded to the primary load carrying metal structure.[1,2] A simplified sketch of a TPS panel is shown in Fig. 1. The aeroelastic or "flutter" behavior of these panels has been investigated in Refs. (2,3). We will focus our main attention on the panel response problems.

The load carrying stiffened metallic panel is modeled as an orthotropic plate. The ceramic tile is modeled by classical thin plate theory while the strain isolator is taken as a linear elastic Winkler foundation.[4] The basic analytical approach in formulating the governing equations of motion uses a Rayleigh-Ritz technique. Then, by determining the relevant energies of the panel components and virtual work due to the random acoustic pressure, the necessary equations of motion are obtained by utilizing Lagrange's equation.

The pressure field is considered as a stationary Gaussian random process for which the cross-correlation function (and/or cross-spectral density) is known empirically from experimental measurements. For the numerical calculations the random acoustic pressure is assumed to be uniform in span-wise direction and convected as random plane waves in the

streamwise direction. When the Rayleigh-Ritz type solution is imposed, cross-spectral density of the generalized random forces is determined. This cross-spectral density is used directly as an input for frequency domain panel response calculations.[5,6] For the time domain approach, it is necessary to have time histories of the generalized random forces. For this purpose, the simulation techniques of random processes are utilized.[6,7,8,9] To reduce computation time, Fast Fourier Transform (FFT) techniques are introduced.[8,9]

When the frequency domain analysis is employed, the response of the panel is determined using standard methods from the theory of random processes.[10-12] By introducing systematic symplifications in this approach, useful explicit analytical formulae for panel response are constructed. These results are then compared with the results obtained by more elaborate techniques such as time domain analysis and finite elements.[6,13] For particular applications where the simplifying assumptions are not valid, numerical simulation of structural response time histories is used.[6,14] In this case, the panel equations of motion are solved numerically on a digital computer in a Monte Carlo sense.

The numerical results include the rms values, time histories and spectral density of the panel response. Stress in the tiles is also calculated. These results then will be compared with the experimental results, which are being conducted at Langley Research Center, NASA.

2. Analysis

2.1 Equations of Motion

The basic analytical approach in formulating the governing equations of motion of a multi-component panel shown in Fig. 1 involves determining relevant energies and virtual work.[2,3] In Ref. 2 the main load carrying metallic substructure was analyzed as an orthotropic plate with simply supported edges while in Ref. 3 the metallic substructure was idealized as an isotropic plate supported by discrete stiffeners and/or point spring supports. In the present study, the main metallic substructure is taken as an orthotropic plate while the ceramic insulation tile is modeled by the classical thin plate theory. The modeling of the strain isolator is more difficult and for more detailed discussion see Ref. 2. For the purpose of this study, the strain isolator is represented by a linear elastic Winkler foundation. In developing the governing equations of motion for the multi-component panel the plate deflection, w^M, and the tile deflection, w^T, are expanded in terms of the trial modes

$$w^M = \sum_{k_x} \sum_{k_y} b_{k_x k_y}(t)\psi_{k_x}(x)\psi_{k_y}(y) \tag{1}$$

$$w^T = \sum_{i_x} \sum_{i_y} a_{i_x i_y}(t)\phi_{i_x}(x)\phi_{i_y}(y) \tag{2}$$

in which $b_{k_x k_y}$ and $a_{i_x i_y}$ are the generalized coordinates for the metallic plate and ceramic tile, respectively, ψ_{k_x}, ψ_{k_y} are the trial modes of the metallic plate, and ϕ_{i_x}, ϕ_{i_y} are the trial modes of the tile. After the expressions for elastic energy, kinetic energy and virtual work are determined for the multi-component panel shown in Fig. 1, the Rayleigh-Ritz

procedure and Lagrange's equation are utilized to develop the governing equations of motion. Since this procedure is rather lengthy for the complex structure considered in this study and the key expressions are available in Refs. 2 and 3, these equations are not included here. The result is a set of coupled linear ordinary differential equations in generalized coordinates $b_{k_x k_y}$ and $a_{i_x i_y}$. The coordinate coupling is introduced through the strain isolator.

2.2 Simplified Response Analysis

For the linear case considered in this paper, response calculations can be performed either in the frequency or time domain. For the time domain approach the equations of motion are solved numerically. To obtain preliminary information, first we consider a simplified response analysis in the frequency domain. The treatment follows along the conventional lines of linear structures and stationary random process inputs whose correlation function (and/or power spectral density) is determined from experimental measurements.[5,10,11,12]

In this simplified approach, it is assumed that the mass distribution of the stiffened elastic panel can be represented by an equivalent evenly distributed mass and the addition of ceramic tiles merely increases the total mass of the panel. Furthermore, the tiles are assumed to be rigidly attached to the metallic substructure and they move according to the motion of the metallic substructure. Then, the panel deflection response spectral density can be written as

$$S_w(\omega,x,y) = \sum_j \sum_k \psi_j(x,y)\psi_k(x,y)$$
$$H_j(\omega)H_k(-\omega)S_{jk}(\omega) \qquad (3)$$

in which $S_{jk}(\omega)$ is the input cross-spectral density of generalized random forces (see Sec. 2.3), $H_j(\omega)$ is the transfer function

$$H_j(\omega) \frac{1}{M_j[\omega_j^2 - \omega^2 + 2i\zeta_j\omega\omega_j]} \qquad (4)$$

with M_j being the generalized mass, ζ_j the modal damping coefficients, and ω frequencies in rad/sec. The mean square panel deflection response is determined from

$$w^{M^2}(x,y) = \int_0^\infty S_w(\omega,x,y)\,d\omega \qquad (5)$$

in which S_w is taken to be one-sided.

For the cases when most of the value of the integral given in Eq. 5 comes from the vicinity of the natural frequency ω_j and the input cross-spectral density $S_{ij}(\omega)$ is slowly varying in these vicinities, the white-noise idealization can be assumed to the input spectral density. Furthermore, by taking the damping in the structure to be relatively small and the natural frequencies well separated so that intermodal coupling can be neglected, a simplified expression for the mean square response if obtained.

$$w^{M^2}(x,y) \approx \frac{\pi}{4} \frac{\sum_j \psi_j^2(x,y)}{M_j^2\omega_j^3\zeta_j} S_{jj}(\omega_j) \qquad (6)$$

One sometimes could make a further assumption that the input random pressure loading is perfectly correlated over the

panel surface. This assumption is reasonable when the characteristic length associated with the random input source is large compared to the panel length and width. If the response is dominated by a single mode (both due to random pressure and the static load), the summation in Eq. 6 can be ignored and the result written as

$$w^{M^2}(x,y) = \frac{\pi}{4} \frac{\psi_1^2(x,y) S_p(\omega_1)}{m^2 \omega_1^3 \zeta_1} \frac{[\int\int \psi_1 dxdy]^2}{[\int\int \psi_1^2 dxdy]^2} \tag{7}$$

in which $S_p(\omega)$ is the random pressure spectral density, and m is the mass per unit area. If we desire stress rather than deflection, then it can be shown that analogous to Eq. 7 one obtains

$$\bar{\sigma}^2(x,y) = \frac{\pi}{4} \frac{\sigma_1^2(x,y) S_p(\omega_1)}{m^2 \omega_1^3 \zeta_1} \frac{[\int\int \psi_1 dxdy]^2}{[\int\int \psi_1^2 dxdy]^2} \tag{8}$$

in which σ_1 is the stress due to $w = \psi_1$.

It should be noted that if for a particular application the simplifying assumptions which lead to the analytical results presented in this section must be abandoned, numerical simulation of structural response time histories may be the method of choice.[6,16]

2.3 Simulation of the Generalized Random Forces

The generalized random force due to the acoustic noise pressure acting on the (m,n) tile can be expressed as

$$Q_j^{mn}(t) = \int_0^{a_T} \int_0^{b_T} p^{mn}(t,x,y) \phi_j(x,y) dxdy \tag{9}$$

in which p^{mn} is the random noise pressure at the (m,n) tile. Taking the mathematical expectation of Eq. 9, the correlation

of the generalized random force (autocorrelation if j = k and cross-correlation is j ≠ k) for a (m,n) tile is

$$R_{jk}^{mn}(\tau) = \int_0^{a_T}\int_0^{b_T}\int_0^{a_T}\int_0^{b_T} R_p^{mn}(\tau,\xi,\eta)\,\phi_j(x_1,y_1)\phi_k(x_2,y_2)\,dx_1dx_2dy_1dy_2 \tag{10}$$

in which $\xi = x_1 - x_2, \eta = y_1 - y_2, \tau = t_1 - t_2$, and $R_p^{mn}(\tau,\xi,\eta)$ is the autocorrelation function of $p^{mn}(t,x,y)$.

Applying the Wiener-Khintchine transform to Eq. 10, the cross-spectral densities (spectral density if j = k) of the generalized random forces are

$$S_{jk}^{mn}(\omega) = \int_0^{a_T}\int_0^{b_T}\int_0^{a_T}\int_0^{b_T} S_p^{mn}(\omega,\xi,\eta)\phi_j(x_1,y_1)\,\phi_k(x_2y_2)\,dx_1dy_1dx_2dy_2 \tag{11}$$

in which $S_p^{mn}(\omega,\xi,\eta)$ is the pressure cross-spectral density (the Wiener-Khintchine transform of $R_p^{mn}(\tau,\xi,\eta)$).

The statistics of random pressure $p^{mn}(t,x,y)$ corresponding to rocket engine noise or turbulent boundary layer are usually determined experimentally. Following Refs. 8, 14. the cross-spectral density $S_p^{mn}(\omega,\xi,\eta)$ can be expressed in the following general form

$$S_p^{mn}(\omega,\xi,\eta) = S_p(\omega)\,|\rho(\xi,0,\omega)|\,|\rho(0,\eta,\omega)|\,e^{-i\omega\xi/u_c} \qquad 0 \le \omega < \infty$$

where $S_p(\omega)$ is the spectral density of random pressure fluctuations, $|\rho(\xi,0,\omega)|$ and $|\rho(0,\eta,\omega)|$ are the spatial correlation coefficients corresponding to streamwise and spanwise directions, respectively, and u_c is the convection

velocity. The correlation coefficients for turbulent boundary layer can be expressed as

$$|\rho(\xi,0,\omega)| = e^{-\alpha_1(\omega,u_c)|\xi|} \tag{13}$$

$$|\rho(0,\eta,\omega) = e^{-\alpha_2(\omega,u_c)|\eta|} \tag{14}$$

where the parameters α_1 and α_2 are determined experimentally. Because the absolute values $|\xi| = |x_1 - x_2|$ and $|\eta| = |y_1 - y_2|$ appear in the exponent of Eqs. 13 and 14, the integration in Eq. 11 has to be carried out over two ranges for both ξ and η, i.e., for $x_1 > x_2$, $x_1 < x_2$ and for $y_1 > y_2$, $y_1 < y_2$.

Time histories of the generalized random forces can be determined from Eq. 9 by simulating the random pressure $p^{mn}(t,x,y)$ as a multidimensional process in space-time domain[7,8]

$$p^{mn}(t,x,y) = \sqrt{2} \sum_{i=1}^{N_1} \sum_{j=1}^{N_2} \sum_{r=1}^{N_3} [S_p^{mn}(\omega_i,k_{1j},k_{2r})\Delta\omega\Delta k_1\Delta k_2]^{1/2} \tag{15}$$

$$\cdot \cos(\omega_i t + k_{1j}x + k_{2r}y + \varphi_{ijr})$$

In Eq. 15, $S_p^{mn}(\omega,k_1k_2)$ is the three-dimensional spectral density (the Wiener-Khintchine transform of $S_p^{mn}(\omega,\xi,\eta)$ on ξ and η) corresponding to random pressure $p^{mn}(x,y,t)$, i.e.,

$$S_p^{mn}(\omega,k_1,k_2) = \frac{4}{(2\pi)^2} \int_0^\infty \int_0^\infty S_p(\omega,\xi,\eta) e^{-j(k_1\xi+k_2\eta)} d\xi d\eta, \tag{16}$$

$\Delta\omega = 2\omega_u/N_1$, $\Delta k_1 = 2k_{1u}/N_2$, $\Delta k_2 = 2k_{2u}/N_3$ with ω_u, k_{1u} and k_{2u} being the upper cutoff frequency and wave numbers, respectively, φ_{ijr} are the random phase angles uniformly distributed between 0 and 2π. From Eqs. 12,13,14 and 16,

the three-dimensional spectral density is

$$S_p^{mn}(\omega,k_1k_2) = \frac{S_p(\omega)\alpha_1(\omega,u_c)\alpha_2(\omega,u_c)}{\pi^2[\alpha_1^2(\omega,u_c) + (\omega/u_c + k_1^2)^2][\alpha_2^2(\omega,u_c) + k_2^2]} \tag{17}$$

On substituting the simulated random process from Eq. 15 into Eq. 9, the generalized random force can be expressed as

$$Q_{sq}^{mn}(t) = (2)^{1/2} \sum_{i=1}^{N_1} (G_{sqi}^{mn} \cos \omega_i t - H_{sqi}^{mn} \sin \omega_i t) \tag{18}$$

where

$$G_{sqi}^{mn} = \sum_{j=1}^{N_2} \sum_{r=1}^{N_3} A^{mn}(\omega_i,k_{1j},k_{2r})(B_{sqjr} \cos \varphi_{jri} - D_{sqjr} \sin \varphi_{jri}) \tag{19}$$

$$H_{sqi}^{mn} = \sum_{j=1}^{N_2} \sum_{r=1}^{N_3} A^{mn}(\omega_i,k_{1j},k_{2r})(B_{sqjr} \sin \varphi_{jri} + D_{sqjr} \cos \varphi_{jri}) \tag{20}$$

$$A^{mn}(\omega_i,k_{1j},k_{2r}) = [S_p^{mn}(\omega_i,k_{1j},k_{2r})\Delta\omega\Delta k_1\Delta k_2]^{1/2} \tag{21}$$

$$B_{sqjr} = U_{sj}\bar{U}_{qr} - V_{sj}\bar{V}_{qr} \tag{22}$$

$$D_{sqjr} = \bar{U}_{qr}V_{sj} + \bar{V}_{qr}U_{sj} \tag{23}$$

$$U_{sj} = \int_o^{a_T} \cos k_{2j}x\phi_s(x)dx \tag{24a}$$

$$\bar{U}_{qr} = \int_o^{b_T} \cos k_{1q}y\phi_r(y)dy \tag{24b}$$

$$V_{sj} = \int_0^{a_T} \sin k_{2j}x\phi_s(x)dx \tag{24c}$$

$$\bar{V}_{qr} = \int_0^{b_T} \sin k_{3q}y\phi_r(y)dy \tag{24d}$$

For the purpose of this study, the trial modes of the individual ceramic tiles were taken to be those of a free-free beam

$$\begin{aligned}\phi_s(x) &= 1, \quad s = 1\\ &= \sqrt{3}\,(1 - 2x/a_T), \quad s = 2\\ &= \cosh \beta_s x + \cos \beta_s x - \alpha_s(\sinh \beta_s x\\ &\quad + \sin \beta_s x), \quad s = 3,4 \ldots\end{aligned} \tag{25}$$

where $\beta_s = 0.0, 0.0, 4.73, 7.85, \ldots$; $\alpha_3 = 0.9825$, $\alpha_4 = 1.0008$, $\alpha_5 = 1.0000$, ... From Eqs. 24 and 25, it can be shown that

$$U_{sj} = \frac{1}{\beta_s^4 - k_{2j}^4}\left[(-1)^s \eta'''_{jc}\big|_{x=a_T} - (-1)^s \alpha_s \beta_s \eta''_{jc}\big|_{x=a_T}\right.$$

$$\left. + \eta'''_{jc}\big|_{x=0} + \alpha_s \beta_s \eta''_{jc}\big|_{x=0}\right] \tag{26}$$

where $\eta_{jc} = \cos k_{2j}x$ and a prime indicates derivative. The values for $\bar{U}_{qr}$, V_{sj} and $\bar{V}_{qr}$ can be obtained in a similar fashion by appropriately adjusting the function η and the limits of integration. It should be noted that when $s = 2$, Eq. 26 need to be multiplied by $\sqrt{3}$.

An alternative method to generate time histories of generalized random forces is to utilize the expression for the cross-spectral density given in Eq. 11, the simulation procedures of multivariate random processes, and the Fast Fourier

Transform (FFT) algorithm.[7,8,9] Then, the generalized random force can be simulated directly as

$$Q_j^{mn}(t) = \mathrm{Re}\{(2\Delta\omega)^{1/2} \sum_{s=1}^{j} \sum_{r=1}^{N_1} |t_{js}(\omega_r)| \, e^{-i[\theta_{js}(\omega_r) + \varphi_{sr}]} e^{i2\pi rk/N_1}\}$$

$$k = 0,1\ldots,N_1-1 \qquad (27)$$

in which Re denotes the real part and

$$\theta_{js}(\omega_r) = \tan^{-1} \frac{\mathrm{Im}[t_{js}(\omega_r)]}{\mathrm{Re}[t_{js}(\omega_r)]} \qquad (28)$$

The elements, t_{js}, of the lower triangular matrix [T] can be obtained from the cross spectral density matrix $[S^{mn}]$ given in Eq. 11 in the following fashion

$$[S^{mn}] = [T][T^*]' \qquad (29)$$

where the asterisk indicates the complex conjugate and a prime denotes matrix transposition.

2.3.1 Spatially Uniform Pressure

Consider the acoustic pressure acting on the panel to be uniformly distributed with respect to spatial coordinates (x,y) and varying randomly in time. For this case, due to the orthogonality principle, only the first tile mode contributes to the generalized random force. Then the cross-spectral density of the generalized random force reduces to

$$S_{jk}^{mn}(\omega) = a_T^2 b_T^2 S_p^{mn}(\omega) \qquad j = k = 1 \qquad (30)$$

$$= 0 \quad \text{otherwise}$$

and the time history of the generalized random force can be simulated from

$$Q_j^{mn}(t) = a_T b_T \sqrt{2} \sum_{i=1}^{N_1} [S_p^{mn}(\omega_i)\Delta\omega]^{1/2} \cos(\omega_i t + \varphi_i) \quad \text{for } j = 1 \qquad (31)$$

$$= 0 \quad \text{otherwise}$$

2.3.2 Convected Random Pressure

Consider the acoustic pressure to be uniform in the spanwise direction and convected as random plane waves in the streamwise direction. The cross-spectral density in this case can be expressed as[15]

$$S_p^{mn}(\xi,\omega) = S_p^{mn}(\omega) \exp(i\omega\xi/u_c) \qquad (32)$$

in which u_c is the convection speed of the random plane waves. From Eqs. 11,25 and 32, it can be shown that

$$S_{jk}^{mn}(\omega) = S_p^{mn}(\omega) b_T^2 a_T^2 [J_{jk}(\omega) + iK_{jk}(\omega)] \qquad (33)$$

in which

$$J_{jk}(\omega) = I_c^j I_c^k + I_s^j I_s^k \qquad (34a)$$

$$K_{jk}(\omega) = I_s^j I_c^k - I_c^j I_s^k \qquad (34b)$$

$$I_{c,s}^j = \{\lambda_{c,s}'' \phi_j' \Big|_0^{a_T} - \lambda_{c,s}''' \phi_j' \Big|_0^{a_T}\} / (\beta_j^4 - \alpha^4)$$

$$\lambda_c'' = -\alpha^2 \cos(\alpha x/a_T), \quad \lambda_s''' = \alpha^3 \sin(\alpha x/a_T) \qquad (35)$$

$$\lambda_s'' = -\alpha^2 \sin(\alpha x/a_T), \quad \lambda_s''' = -\alpha^3 \cos(\alpha x/a_T)$$

with $\alpha = -a_T/U$ and a prime indicating a derivative ($' \equiv d/d(x/a_T)$). It should be noted that when

Mode j symmetric, mode k antisymmetric, $J_{jk} = 0$

Mode j symmetric, mode k symmetric, $K_{jk} = 0$

Mode j antisymmetric, mode k antisymmetric, $K_{jk} = 0$

and $J_{jk} = J_{kj}$, $K_{jk} = - K_{kj}$. Then, the time histories of the generalized random forces due to convected pressure can be generated from Eqs. 27 and 33.

2.4 Response Simulation

For the time domain approach, the governing differential equations of motion are combined with the time histories of the generalized random forces given in Eqs. 18 or 27. Utilizing a step-by-step temporal numerical integration and modal expansion for panel and tile deflections presented in Eqs. 1 and 2, time histories of $w^M(x,y,t)$ and $W^T(x,y,t)$ are determined. By assuming the response process to be ergodic, the mean square response can be obtained using the temporal average. For example, the mean square response of the metallic panel deflections is

$$\overline{w^M}^2(x,y) = \frac{1}{T_o} \int_o^{T_o} (w^M(t,x,y))^2 dt \tag{36}$$

in which T_o is the sample duration. The panel deflection response spectral density, S_w, can be calculated utilizing the Fast Fourier Transform (FFT) algorithm on the response history $w^M(x,y,t)$. The numerical estimate of spectral density at frequency ω is

$$S_w(x,y,\omega_k) = \frac{2}{N\Delta t} Y_w(x,y,\omega_k)^2 \tag{37}$$

where

$$Y_w(x,y,\omega_k) = \sum_{n=0}^{N-1} w^M(x,y,t_n)\exp(-i2\pi kn/N)$$

$$k = 1,2\ldots,N \qquad (38)$$

with Δt being the time increment and N the number of simulated points.

The stress response in the metallic plate and the supporting stringers can be determined from the information on the curvature corresponding to deflection $w^M(x,y,t)$. For example, the maximum stress in the stringer can be estimated from

$$\sigma_{sT} = E_M d^* \frac{\partial^2 w^M}{\partial x^2} \qquad (39)$$

where d^* is the maximum distance between the centroid of the cross-section and outer edge of the stringer and E_M is the elastic modulus of the stringer. Similarly, the maximum bending stress in the tile is conservatively estimated by assuming the tile bonds with the metallic plate,

$$\sigma_{Tile} = E_T \frac{t_T}{2} \frac{\partial^2 w^T}{\partial x^2} \qquad (40)$$

where t_T and E_T are thickness and elastic modulus of the tile, respectively. The normal stress in the tile can be calculated

$$\sigma^n_{Tile} = \frac{E_{z_I}}{t_I}(w^M - w^T) \qquad (41)$$

in which E_I and t_I are the elastic modulus and thickness of the strain isolator, respectively.

3. Numerical Results

3.1 Simplified Frequency Domain Analysis

As an example consider an orthotropic panel (with and without tiles) as shown in Fig. 1. It is assumed that tiles follow the metallic panel motion and are rigidly attached to the metallic panel. The physical data for this panel is given in Table I. Consider this panel to be loaded by the acoustic random pressure for which the suggested power spectral density is given in Fig. 2.

3.1.1 Uniform Pressure

Assume the acoustic noise pressure to be fully correlated in space over the panel surface. The aluminum panel and the tiles have the following properties: $E_M = 10.5 \times 10^6$ psi, $E_T = 34 \times 10^3$ psi, $a_T = 6$ in, $a = 8a_T$, $a^* = 37$ in (distance between the line supports), $b_T = 6$ in, $b = 3b_T$, $d^* = 0.972$ in (maximum stringer depth measured from the neutral axis of plate-stringer combination) $m_M = 0.0083/386$ (lb-sec^2/in^3), $\rho_T = 9$ lb/ft^3. The mass, the natural frequencies, and the respective pressure spectral densities at these frequencies, corresponding to the first streamwise bending mode are

$m_M = 0.0083/386$ (lb-sec^2/in^3), $\omega_1 = 716$ rad/sec,
$S_p(\omega_1) = 2.5 \times 10^{-4}$ (psi)^2-sec/rad (no tiles);

$m_{M+T} = 0.01351/386$ (lb-sec^2/in^3), $\omega_1 = 571$ rad/sec,
$S_p(\omega_1) = 2.78 \times 10^{-4}$ (psi)^2-sec/rad (1" tiles);

$m_{M+T} = 0.01663/386$ (lb-sec^2/in^3), $\omega_1 = 502$ rad/sec,
$S_p(\omega_1) = 2.80 \times 10^{-4}$ (psi)^2-sec/rad (1.6" tiles);

$m_{M+T} = 0.02030/386$ (lb-sec^2/in^3), $\omega_1 = 452$ rad/sec, $S_p(\omega_1) = 2.95 \times 10^{-4}$ (psi)^2-sec/rad (2.3" tiles). The panel shown in Fig. 1 has an overhang of 5.5 in at both ends. The approximate modes that are chosen for the simplified frequency domain analysis correspond to the panel length between the line supports, i.e., $a^* = 37$ in. It is assumed that the response is dominated by the fundamental vibration mode so that Eqs. 7 and 8 can be applied. The response calculations are performed first by assuming the panel to be free at the edges $y = 0,b$ and simply supported along the line supports. Corresponding to these support conditions, the first natural panel vibration mode can be taken as

$$\psi_1(x,y) = 1 \cdot \sin \frac{\pi x}{a^*} \tag{42}$$

Assuming the same free support boundary conditions at the edges $y = 0,b$, but clamped supports along the line supports, the first vibration mode can be approximated by

$$\psi_1(x,y) = 1 \cdot \left(1 - \cos \frac{2\pi x}{a^*}\right) \tag{43}$$

Then, utilizing these conditions and Eqs. 7 and 8, the root mean square response can be determined. The rms values of deflection, stringer stress and stringer strain are shown in Table II at the middle of the panel, i.e., $y = b/2$, $x = a^*/2$.

3.1.2 Convected Pressure

Consider the convected acoustic random pressure characterized by the cross-spectral density of the following form[15]

$$S_p(\omega,\xi) = S_p(\omega) \cos \frac{\omega\xi}{u_c} \tag{44}$$

Then, the effect of the spatial correlation can be included by multiplying Eqs. 7 and 8 by the following factor

$$R^2 = \frac{\int_0^{a^*}\int_0^{a^*} \cos \frac{\omega}{u_c}(x_1 - x_2)\psi_1(x_1)\psi_1(x_2)dx_1dx_2}{[\int_0^{a^*} \psi_1(x)dx]^2}$$

Substituting Eqs. 42 and 43 into Eq. 45 and integrating, we obtain

$$R^2 = \frac{(\pi/a^*)^4(1 + \cos \frac{\omega a^*}{u_c})}{2[(\pi/a^*)^2-(\omega/u_c)^2]^2} \tag{46}$$

for free-simple supports, and

$$R^2 = \frac{2}{\alpha^{*2}}(1 - \cos \frac{\omega a^*}{u_c})(\frac{u_c}{\omega} - \frac{u_c a^{*2}\omega}{(a^*\omega)^2 - (2\pi u_c)^2})^2 \tag{47}$$

for free-clamped supports. The values for the reduction factor, R, corresponding to the case where u_c is equal to the speed of sound at the sea level, i.e., u_c = 13,210 in/sec, are given in Table III. The rms values of deflection, stringer stress and stringer strain due to a convected random pressure are shown in Table IV.

3.2 Simulation Analysis

3.2.1 Assumed Sound Pressure Level

Space shuttle panel response calculations were performed in time domain due to acoustic sound pressure near the base of the orbiter at shuttle lift-off. The generalized random forces were generated in time domain using Eqs. 27 and 33. The sound pressure spectral density $S_p^{mn}(\omega)$ is given

in Fig. 2. It is assumed that each tile has an identical sound pressure spectral density, i.e., $S_p^{mn}(\omega) = S_p(\omega)$. Thus, in Eq. 33 a_T is replaced by a and b_T by b. Numerical computations are limited to four streamwise (lengthwise) modes and one spanwise (widthwise) mode. To simulate the translational elastic supports in the spanwise direction (Fig. 1), twenty points at x = 5.5 in and x = 42.5 in across the panel were chosen. At each point an elastic translational spring with stiffness of 1×10^4 lb/in was assumed to be attached. Simulation of the generalized random forces was accomplished utilizing the following data: u_c = 13,210 in/sec, N_1 = 512, $\omega_u = 2\pi \times 1000$ rad/sec. It was assumed that damping in each mode was the same.

The simulated time histories of the generalized random forces corresponding to convected random sound pressure are given in Ref. 6 for the first four free-free beam vibration modes. A portion of the deflection response history at the middle of the panel to which the 2.3" ceramic tiles are attached is given in Fig. 3 where the nondimensional time, τ, is

$$\tau = t(D_x/ma^4)^{1/2} .$$

The root mean square response corresponding to panel deflection, stress and strain in the stringer at x/a = 0.5 and y/b = 0.5 is presented in Table V for a combination of several tile thicknesses and damping coefficients. The normal stresses in each tile (Eq. 41) along the centerline of the panel are shown in Fig. 4.

3.2.2 Experimental Sound Pressure Level

Input random sound pressure spectral and cross-spectral densities were measured at the Langley, NASA, progressive wave acoustic tunnel. These measurements were obtained for 140 dB, 150 dB and 160 dB over-all sound pressure levels. Typical results of the pressure spectal density at the middle of the panel at 150 dB and 160 dB levels are shown in Figs. 5 and 6. The experimental results indicated no significant decay in the pressure spectral density with respect either to streamwise of spanwise spatial separations. For the purpose of this analytical study, it was assumed that the random pressure is uniform in spanwise direction and convected as random plane waves in the streamwise direction. Utilizing the pressure spectral densities given in Figs. 5 and 6, the generalized random forces were generated in time domain from Eqs. 27 and 33.

In Fig. 7, the strain response time history in the stringer at x/a = .5 and y/b = .5 is shown for a panel with the 2.3" tiles attached corresponding to 160 dB input. Similar results are presented in Fig. 8 for a panel with 1" tiles and pressure input of 150 dB level. The root mean square response of panel deflection, stringer stress and stringer strain is given in Tables VI and VII corresponding to 150 dB and 160 dB inputs, respectively. The stringer strain spectral densities at the middle of the panel are shown in Figs. 9 - 14 for various combinations of damping and tile thickness. A portion of stringer strain response

time history at x/a = 0.3 and y/b = 0.5 is shown in Fig. 15. The stringer strain spectral density corresponding to this time history is given in Fig. 16.

4. Conclusions and Recommendations for Future Work

A simple analytical model which represents the dynamic characteristics of the surface insulation panels for the space shuttle has been developed. Response calculations were performed utilizing a simplified analysis in the frequency domain and a simulation procedure in the time domain. The results indicate that the simplified spectral density approach is sensitive to the type of vibration mode chosen. It tends to underestimate the response for free-fixed mode and to overestimate the response for free-simple mode when compared to the results obtained by the time domain simulation procedure.

The computer time for the simulation analysis is almost negligible. For example, it takes about one minute on the IBM 360/91 to perform one set of calculations. This includes simulating the generalized random forces, numerically integrating the equations of motion, determining the response root mean square values and the response spectral densities.

To improve upon the numerical results, the following recommendations for future work are suggested:

1. Allow the random sound pressure to vary spatially in both the spanwise and streamwise directions. (Include spatial correlations.)

2. Include a possible nonuniformity in the transverse elastic supports.
3. Include torsional restraints in modeling the elastic supports.
4. Model the strain isolator as a nonlinear material.
5. Determine panel response due to boundary layer turbulence during the maximum flight dynamic pressure including the effect of fluid-structure interaction (aeroelasticity).

References

1. Bohon, M. L., "Thermal Protection Systems for Space Shuttle," in D. Greenshields, G. Strouhal, D. Tilliam, J. Pawloski, Development Status of Reusable Non-Metallic Thermal Protection, TMS-2273, April 1971, NASA.

2. Dowell, E. H., "Vibration and Flutter Analysis of Reusable Surface Insulation Panels," Journal of Spacecraft and Rockets, Vol. 12, No. 1, Jan 1975, pp. 44-50.

3. Dowell, E. H., "Theoretical Vibration and Flutter Studies of Point Supported Panels," Journal of Spacecraft and Rockets, Vol. 10, No. 6, June 1973, pp. 389-395.

4. Dowell, E. H., "Dynamic Analysis of an Elastic Plate on A Thin, Elastic Foundation," Journal of Sound and Vibration, Vol. 35, No. 3, 1974, pp. 343-360.

5. Dowell, E. H. and Vaicaitis, R., "A Primer for Structural Response to Random Pressure Fluctuations," AMS Report No. 1220, Princeton University, April 1975.

6. Vaicaitis, R., "Random Input and Response Study of Multi-Component Panels," Technical Report No. 1., Dept. of Civil Engineering and Engineering Mechanics, Columbia University, Prepared for NASA under NSG-1059, July 1975.

7. Shinozuka, M. and Jan, C. M., "Digital Simulation of Random Processes and Its Applications," Journal of Sound and Vibration, Vol. 25, No. 1, 1972, pp. 111-218.

8. Vaicaitis, R., "Generalized Random Forces for Rectangular Panels," AIAA, Journal, Vol. 11, No. 7, July 1973, pp. 984-988.

9. Shinozuka, M., "Digital Simulation of Random Processes in Engineering Mechanics with the Aid of FFT Technique in Stochastic Problems in Mechanics," S. T. Ariaratnam and H.H.E. Liepholz, Editors, University of Waterloo Press, 1974, pp. 277-286.

10. Miles, J. W., "On Structural Fatigue Under Random Loading," J. Aeronautical Sciences, Vol. 21, No. 11, November 1954, pp. 753-762.

11. Powell, A., Chapter 8 in book, Random Vibration, Edited by S. H. Crandall, Technology Press, Cambridge, Mass. 1958.

12. Lin, Y. K., Probabilistic Theory of Structural Dynamics, McGraw-Hill, New York, N.Y. 1967.

13. Ojalvo, I. U. and Ogilvie, P. L., "Modal Analysis and Dynamic Stresses for Acoustically Excited Shuttle Insulation Tiles," Gruman Aerospace Corporation, August 1975.

14. Vaicaitis, R., Dowell, E. H., and Ventres, C. S., "Nonlinear Panel Response by a Monte Carlo Approach," AIAA Journal, Vol. 12, No. 5, May 1974, pp. 685-691.

15. Mercer, C. A., "Response of Multi-Supported Beam to a Random Pressure Field," Journal of Sound and Vibration, Vol. 2, No. 3, 1965, pp. 293-306.

16. Rucker, Carl, NASA Langley Research Center, personal communication.

Acknowledgement

The author wishes to express his gratitude to Professor E. H. Dowell of Princeton University for making it possible to use some of his computer programs.

Table I

Physical Parameters for RSI Panels

Tile		Isolator	
E_T, psi	$24 \pm \frac{5}{10} \times 10^3$	E_{Z_I}, psi	15 ± 10
t_T, in	1, 1.6, 2.3	t_I, in	0.16
ρ_T, #/ft^3	9		
a_T, in	6		
b_T, in	6		

Metallic Panel

E_M, psi	10.5×10^6	a, in	48
ν_M	0.33	b, in	18
ρ_M, #/in^3	0.1	a*, in	37
D_x, #-in	220,000		
D_y, #-in	31		
D_{xy}, #-in	9812 or 3300		
D_1, #-in	9		
Outer fiber location for the stringer from neutral axis, in	0.972		

Table II

Root Mean Square Response to Uniform Pressure.
Simplified Frequency Domain Analysis. Acoustic Launch Loads

Tile Thickness t_T, in	Damping c/c_{cr}	Deflection $\overline{w^M}$, in		Stringer Stress σ_{sT}, psi		Stringer Strain $\varepsilon_{sT} \times 10^4$, in/in	
		support		support		support	
		Free-simple	Free-fixed	free-simple	Free-fixed	free-simple	free-fixed
0	.01	0.435	0.228	31,819	16,656	30.26	15.80
0	.02	0.308	0.161	22,500	11,778	21.40	11.21
1	.01	0.395	0.206	28,842	15,098	27.43	15.47
1	.02	0.279	0.146	20,395	10,676	19.39	10.94
1.6	.01	0.378	0.198	28,506	14,921	27.11	14.62
1.6	.02	0.270	0.140	20,150	10,500	19.11	10.30
2.3	.01	0.346	0.181	25,597	13,399	24.32	12.72
2.3	.02	0.246	0.128	18,100	9,475	17.20	9.00

Table III

Reduction Factor, R, Due to Spatial Correlation

Tile Thickness (in) First Mode Frequency (rad/sec)	R Free-simple support	R Free-fixed support
No tiles $\omega = 714$	0.912	0.936
$t_T = 1$ $\omega = 572$	0.941	0.956
$t_T = 1.6$ $\omega = 503$	0.954	0.968
$t_T = 2.3$ $\omega = 452$	0.960	0.974

Table IV

Root Mean Square Response to Convected Pressure.
Simplified Frequency Domain Analysis. Acoustic Launch Loads

Tile Thickness t_T, in	Damping c/c_{cr}	Deflection $\overline{w^M}$, in		Stringer Stress σ_{sT}, psi		Stringer Strain $\varepsilon_{sT} \times 10^4$, in/in	
		support		support		support	
		free-simple	free-fixed	free-simple	free-fixed	free-simple	free-fixed
0	.01	0.396	0.213	29,018	15,590	27.59	14.79
0	.02	0.281	0.151	20,520	11,024	19.52	10.40
1	.01	0.372	0.197	27,140	14,463	25.81	14.82
1	.02	0.263	0.140	19,192	10,227	18.25	10.48
1.6	.01	0.361	0.191	27,194	14,443	25.86	14.15
1.6	.02	0.262	0.139	19,229	10,213	18.28	10.01
2.3	.01	0.332	0.176	24,573	13,050	23.34	12.39
2.3	.02	0.236	0.125	17,376	9,228	16.51	8.77

Table V

Root Mean Square Response to Convected Random Pressure
at the Middle of the Panel. Time Domain Analysis (Acoustic Launch Loads

Tile Thickness t_T, in	Damping c/c_r	Deflection $\bar{w}^M$, in	Maximum Stringer Stress σ_{sT}, psi	Maximum Stringer Strain $\varepsilon_{sT} \times 10^4$, in/in
0	.005	.580	42,500	40.30
0	.01	.410	30,500	28.65
0	.02	.295	21,600	20.60
1.0	.005	.505	36,200	35.20
1.0	.01	.354	25,600	24.75
1.0	.02	.250	18,140	17.50
1.6	.005	.446	34,200	32.70
1.6	.01	.326	24,200	23.21
1.6	.02	.233	17,120	16.20
2.3	.005	.352	26,200	25.10
2.3	.01	.214	16,200	15.85
2.3	.02	.157	11,700	11.15
2.3	.03	.130	9,700	9.30

Table VI

Root Mean Square Response to Convected
Random Pressure at the Middle of the Panel. Time Domain Analysis
(Experimental Input 150dB/30psi)

Tile Thickness t_T, in	Damping C/C_{cr}	Deflection $\overline{W}^M$, in	Stringer Stress σ_{ST}, psi	Stringer Strain $\varepsilon_{ST} \times 10^4$ in/in
0	.005	.0490	3,579	3.40
0	.01	.0385	2,809	2.67
.5	.005	.0478	3,482	3.3]
.5	.01	.0378	2,753	2.57
1.0	.005	.0420	3,062	2.88
1.0	.01	.0332	2,423	2.27
1.6	.005	.0352	2,569	2.42
1.6	.01	.0286	2,086	1.95
2.3	.005	.0217	1,587	1.41
2.3	.01	.0198	],448	1.35

Table VII

Root Mean Square Response to Convected Random Pressure at the Middle of the Panel. Time Domain Analysis (Experimental Input, 160 dB)

Tile Thickness t_T, in	Damping c/c_r	Deflection $\bar{w}^M$, in	Maximum Stringer Stress σ_{sT}, psi	Maximum Stringer Strain $\varepsilon_{sT} \times 10^4$, in/in
0	.005	.112	8,250	7.85
0	.01	.079	5,860	5.56
0	.02	.056	4,140	3.92
1.0	.005	.103	7,410	6.95
1.0	.01	.072	5,220	4.90
1.0	.02	.051	3,743	3.49
1.6	.005	.105	7,320	6.90
1.6	.01	.071	5,180	4.86
1.6	.02	.051	3,687	3.45
2.3	.005	.079	5,960	5.40
2.3	.01	.056	4,210	3.82
2.3	.02	.040	2,894	2.70
2.3	.03	.033	2,480	2.23

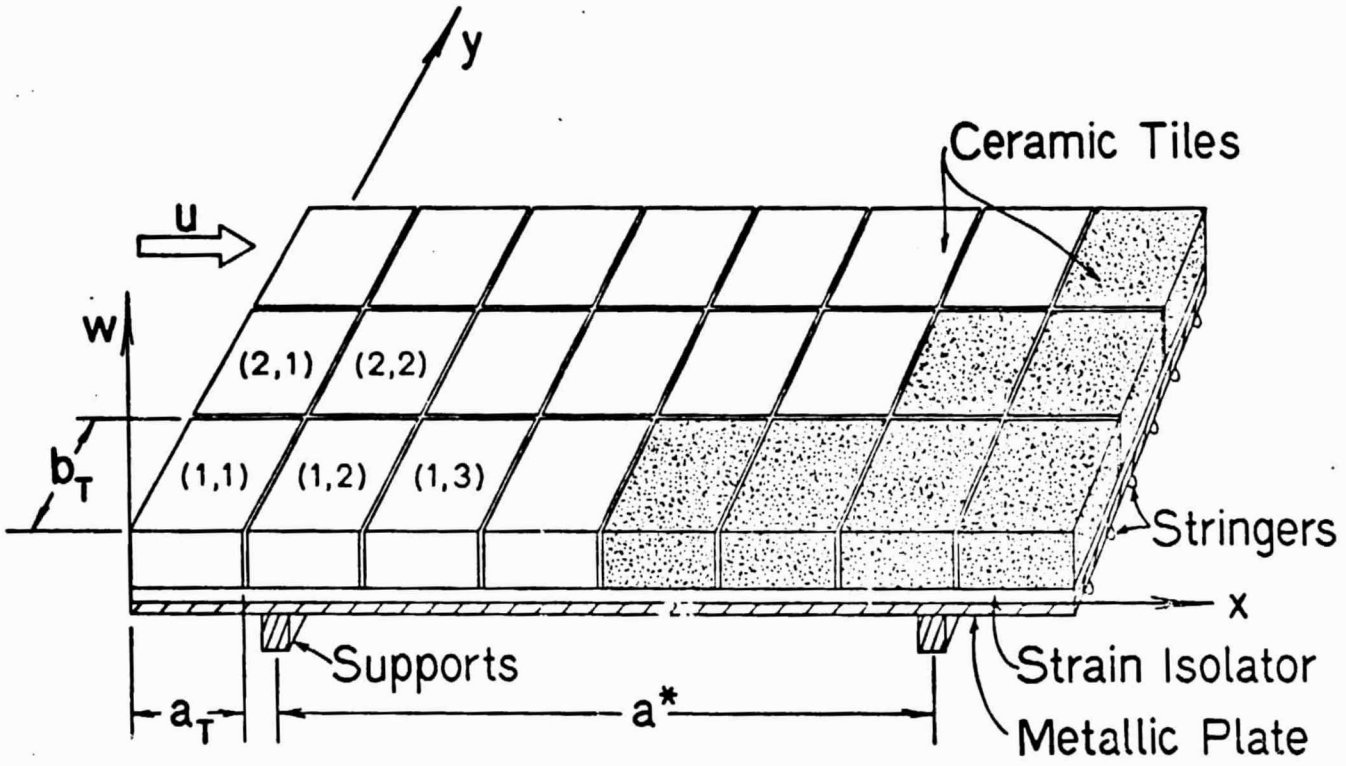

Fig. 1. Model for a Surface Insulation Panel (Space Shuttle)

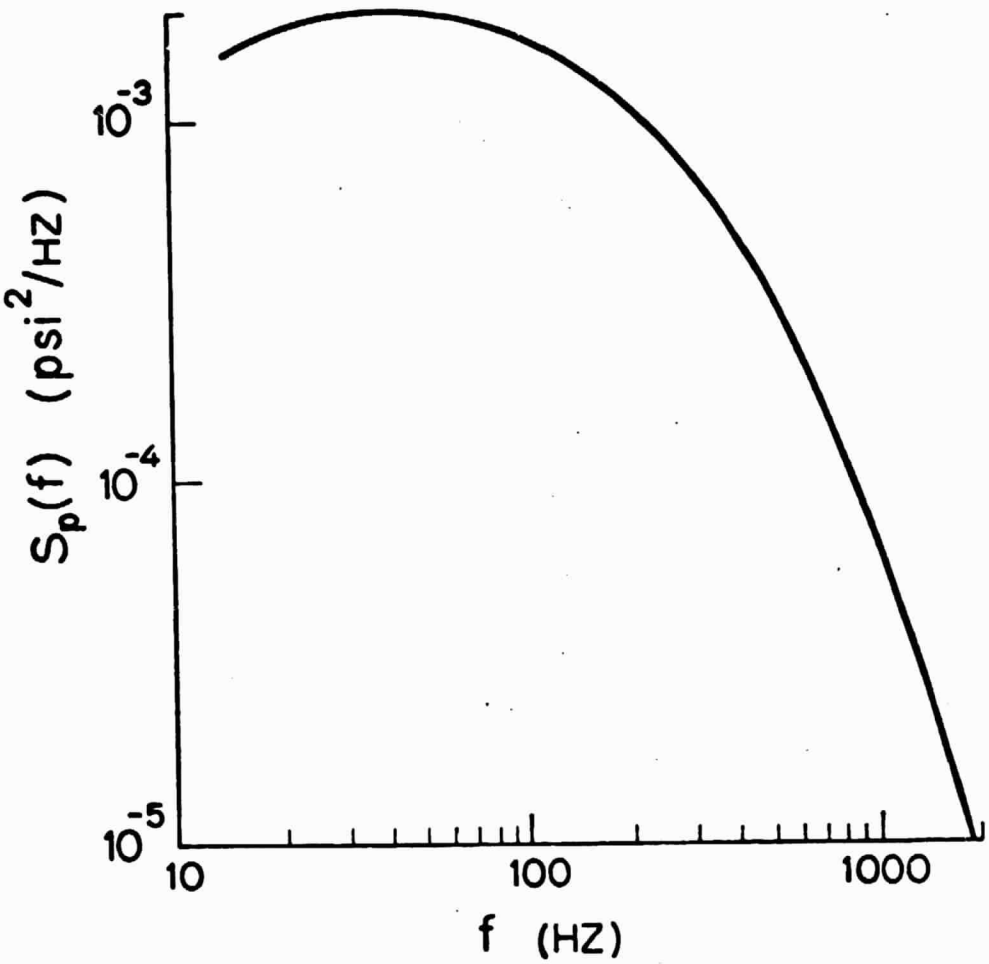

Fig. 2. Assumed Sound Pressure Spectral Density at Shuttle Lift-Off

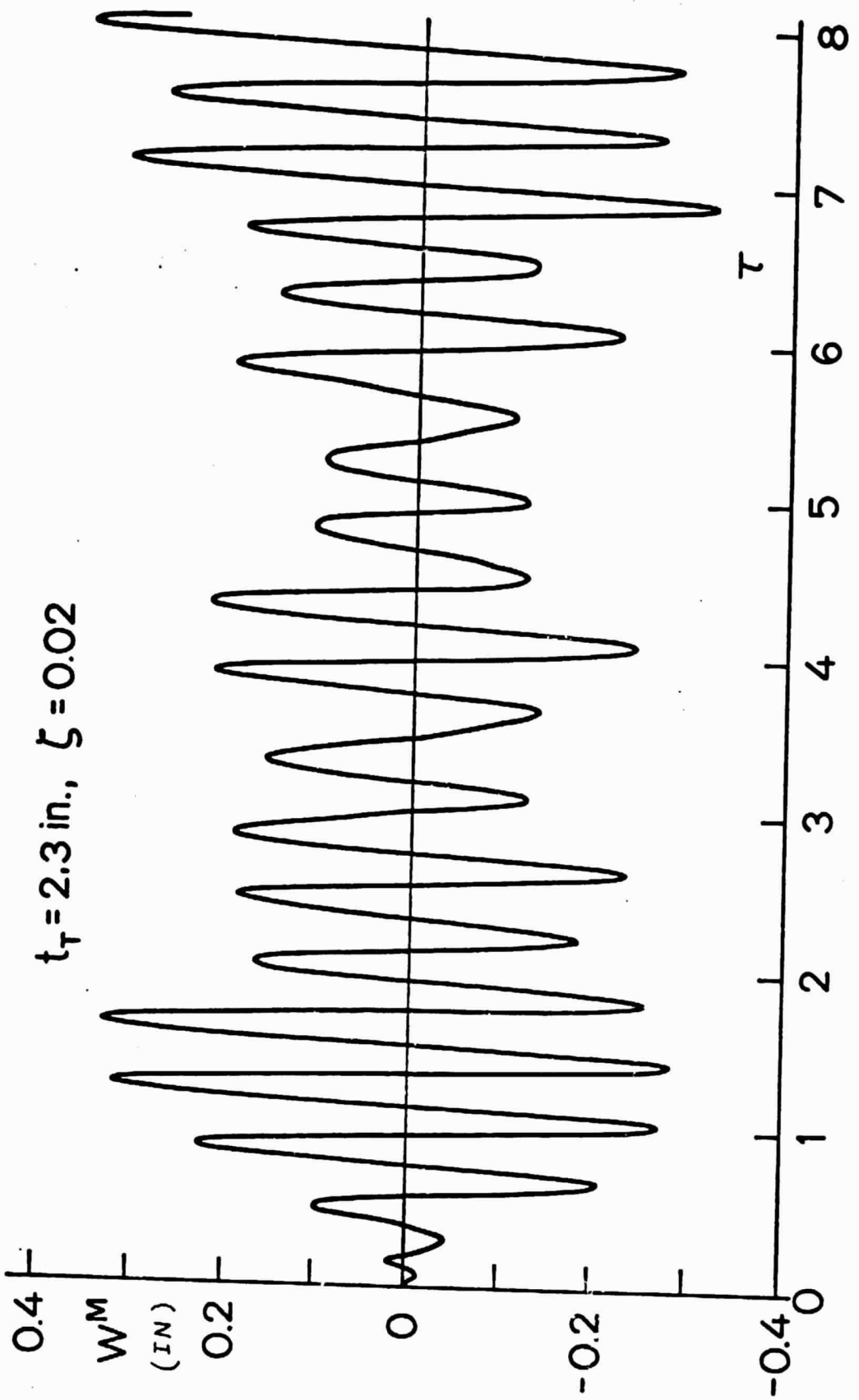

Fig. 3. Deflection Response Time History at the Middle of the Panel

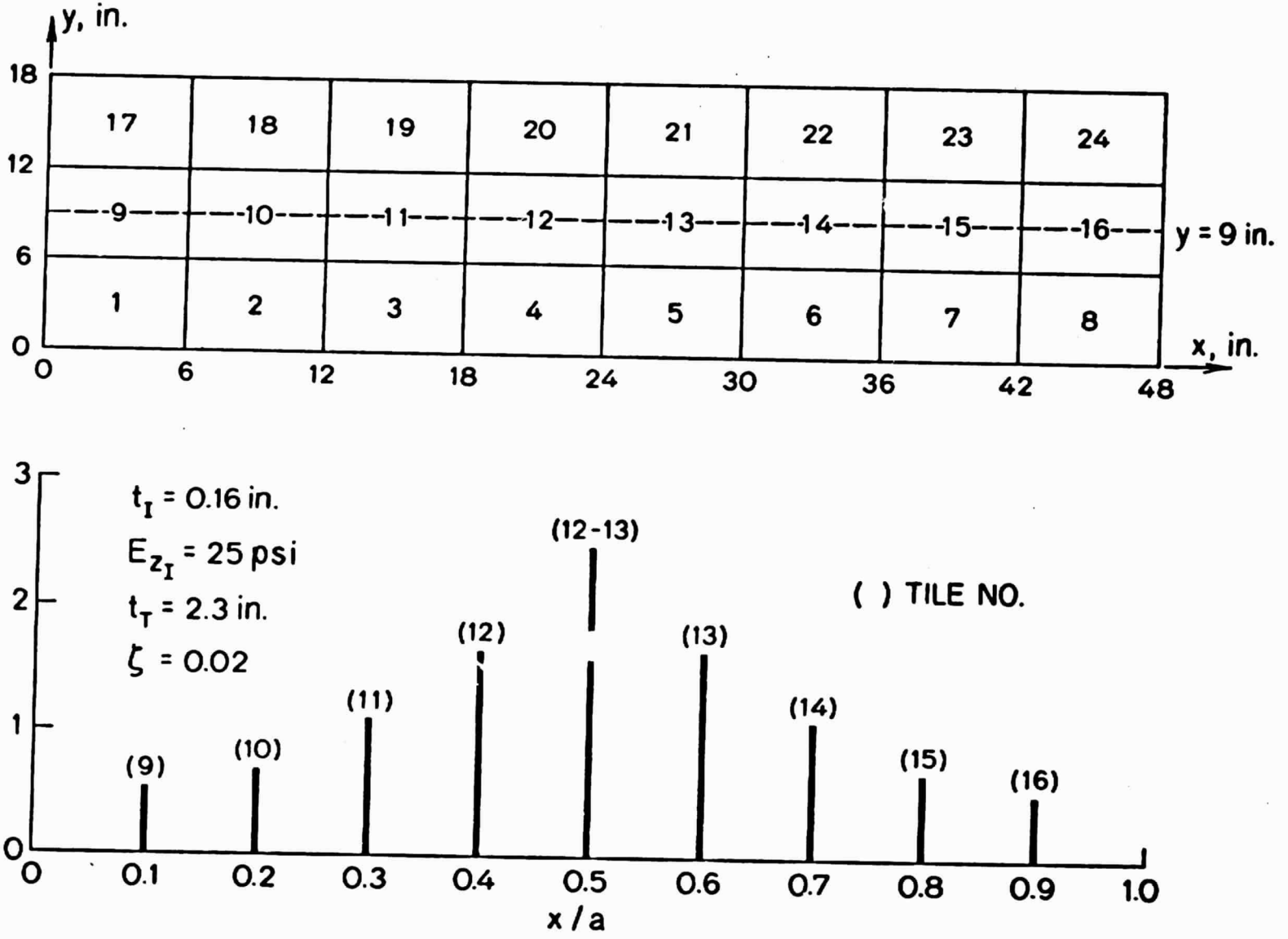

Fig. 4. Normal Stresses in the Tiles. Acoustic Launch Loads

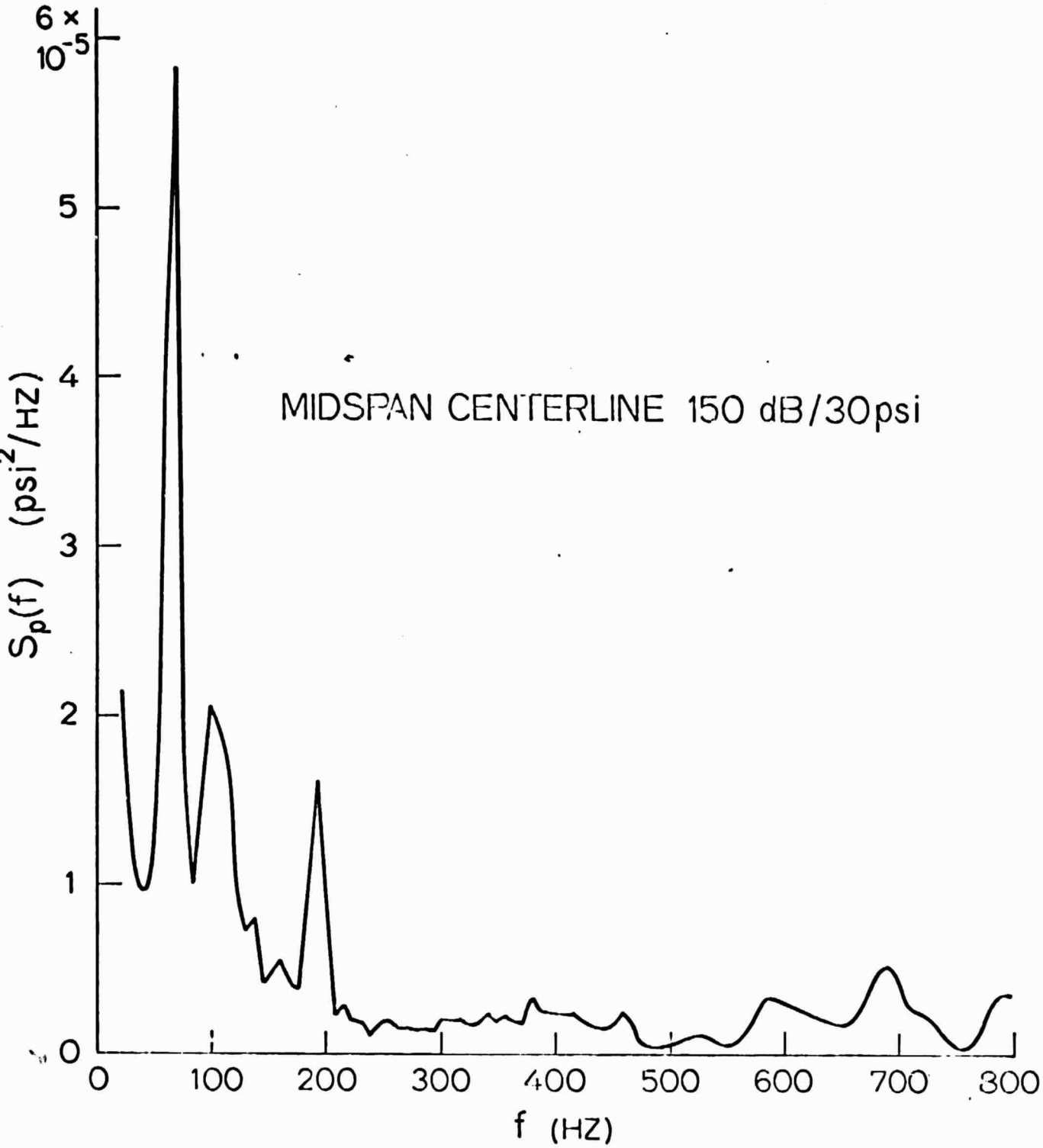

Fig. 5. Experimental Pressure Spectral Density (150 dB)

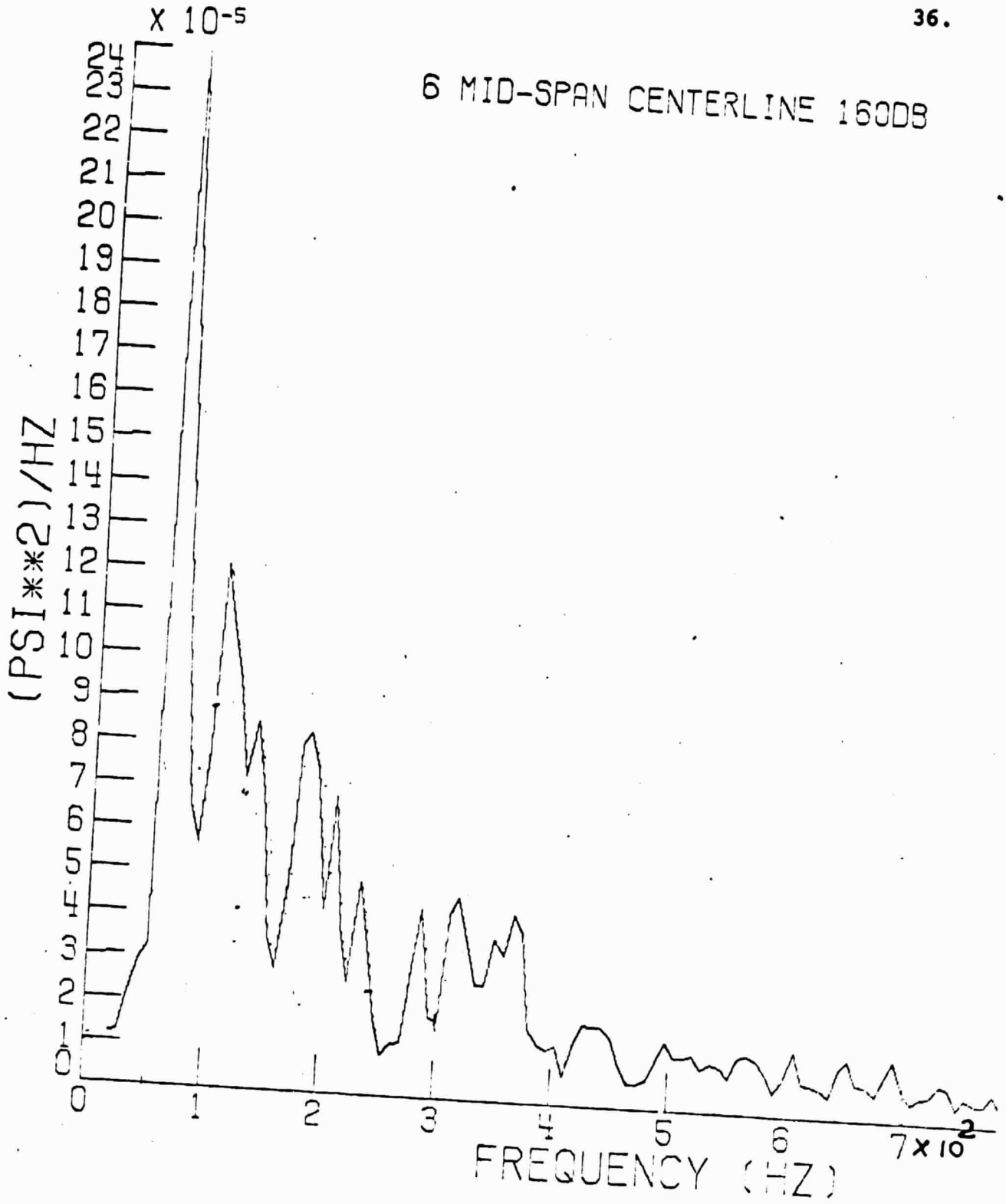

Fig. 6. Experimental Pressure Spectral Density (160 dB)

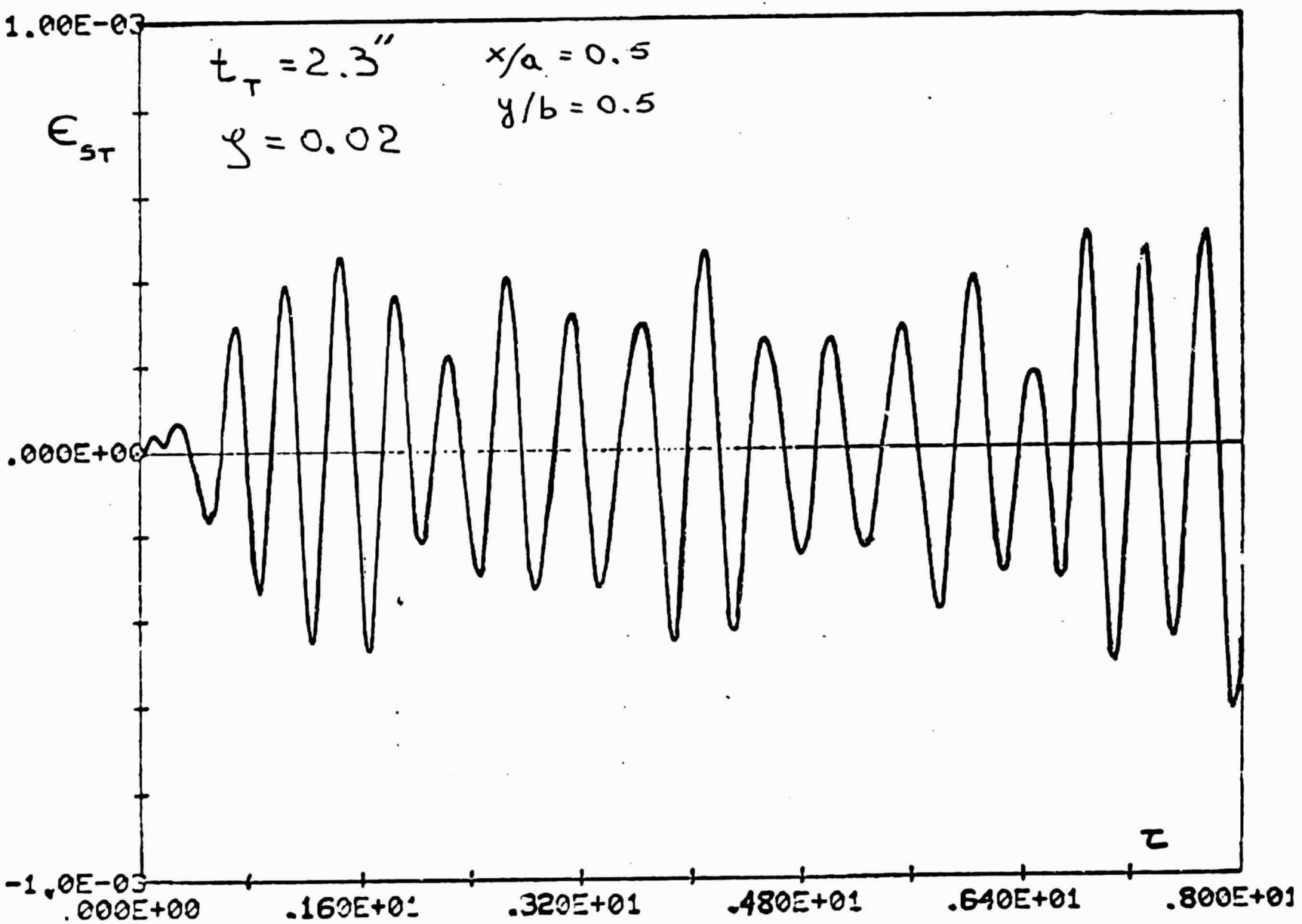

Fig. 7. Stringer Strain Time History (160 dB level Input)

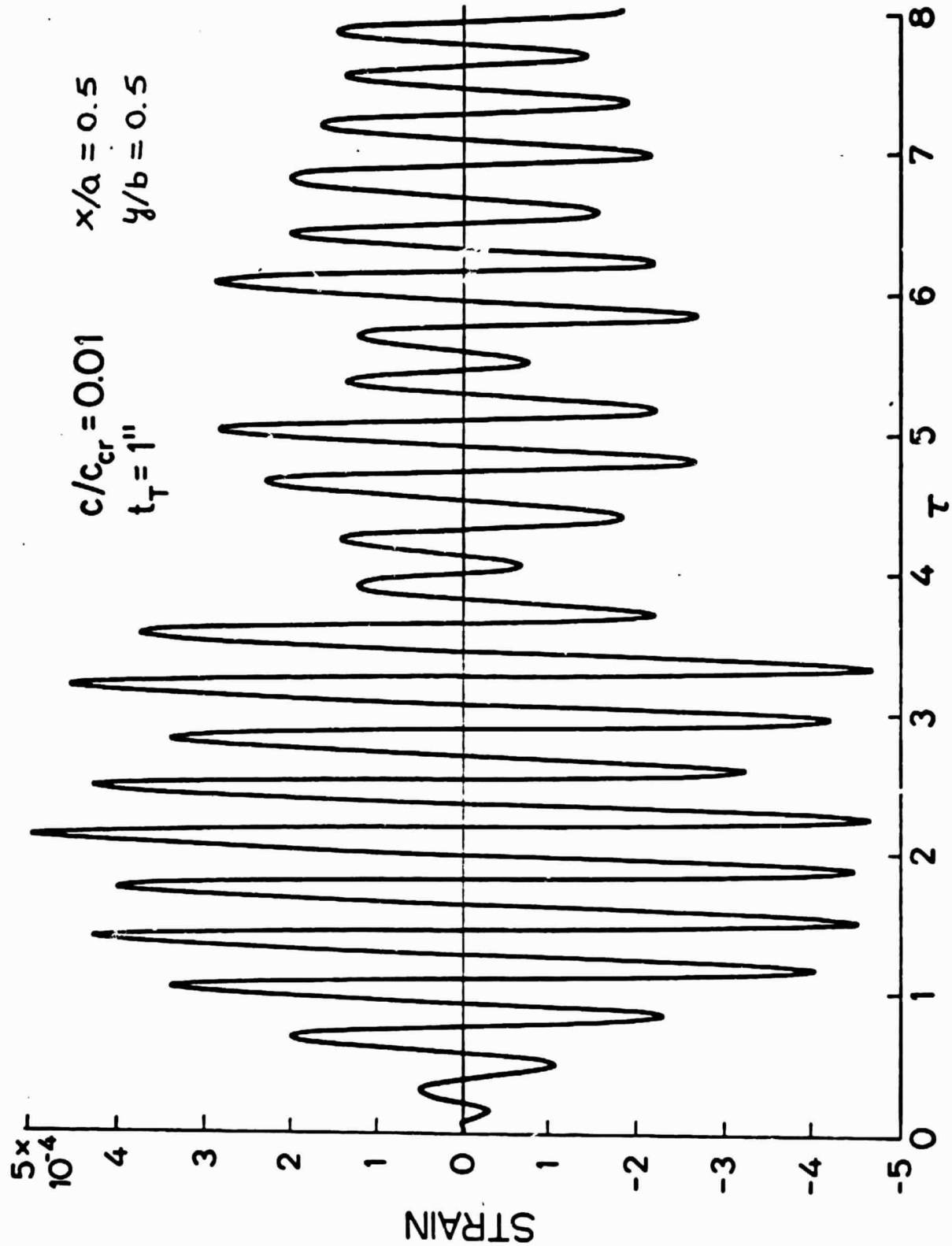

Fig. 8. Stringer Strain Time History (150 dB Level Input)

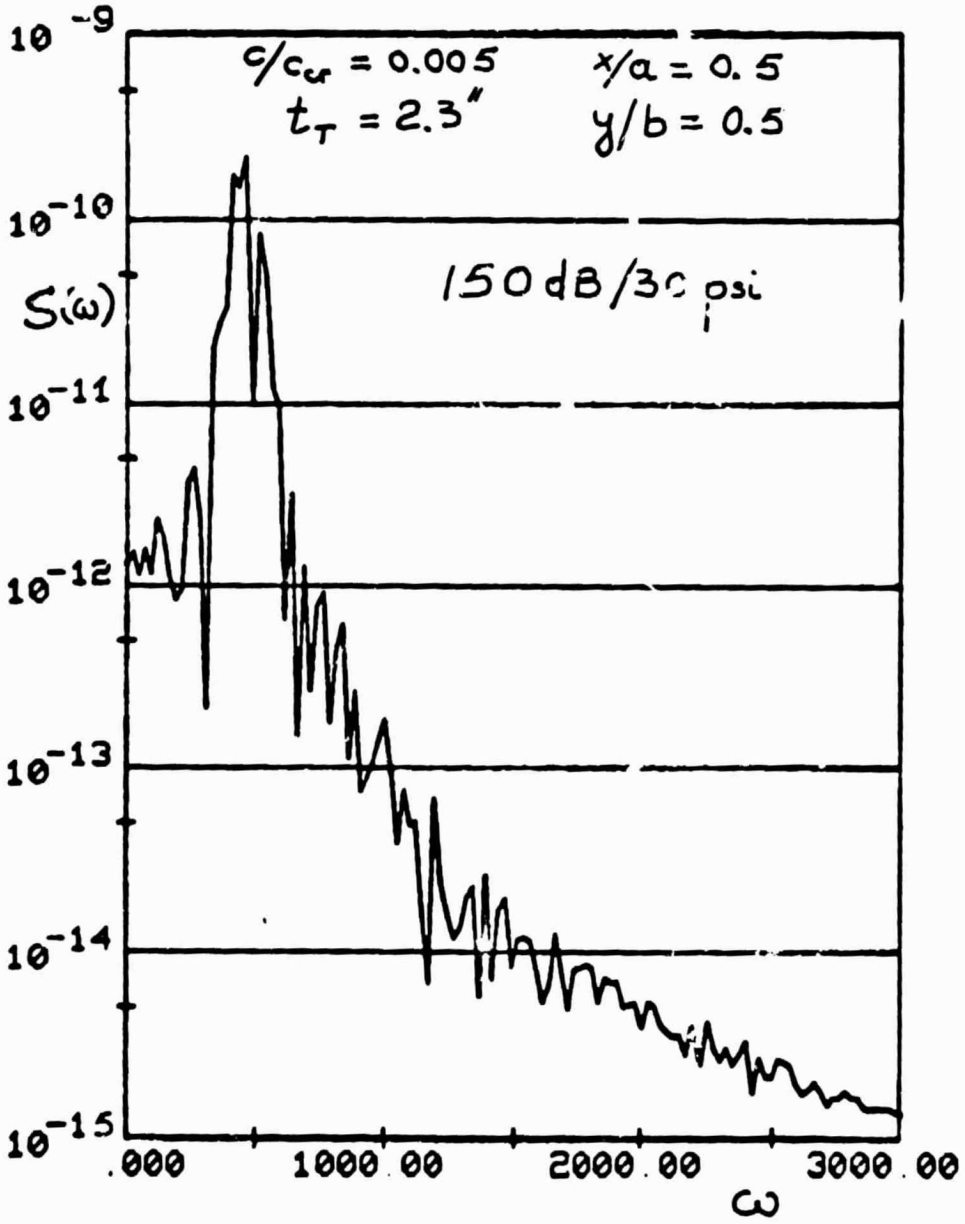

Fig. 9. Stringer Strain Spectral Density (c/c_{cr} = .005, t_T = 2.3")

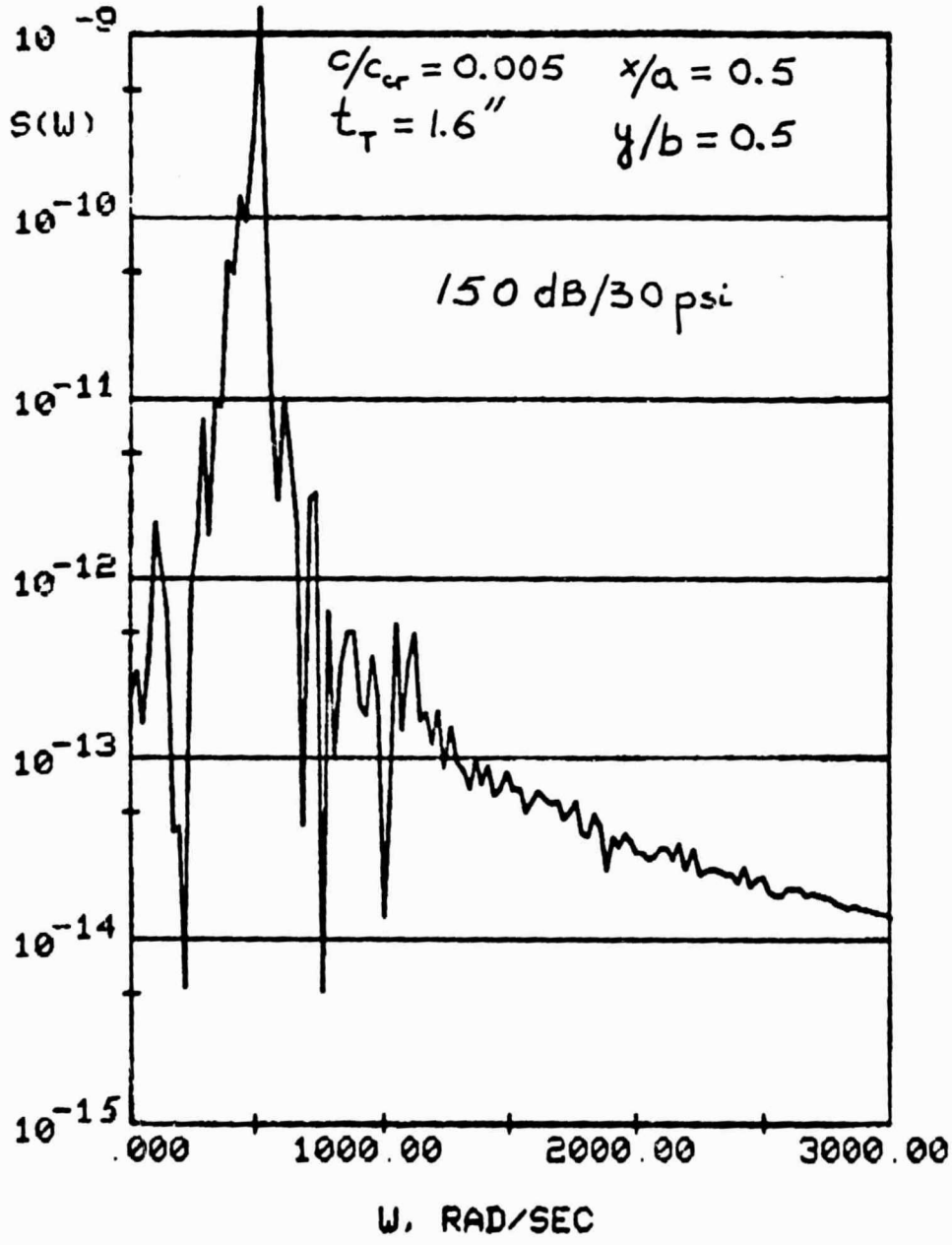

Fig. 10. Stringer Strain Spectral Density (c/c_{cr} = .005, t_T = 1.6")

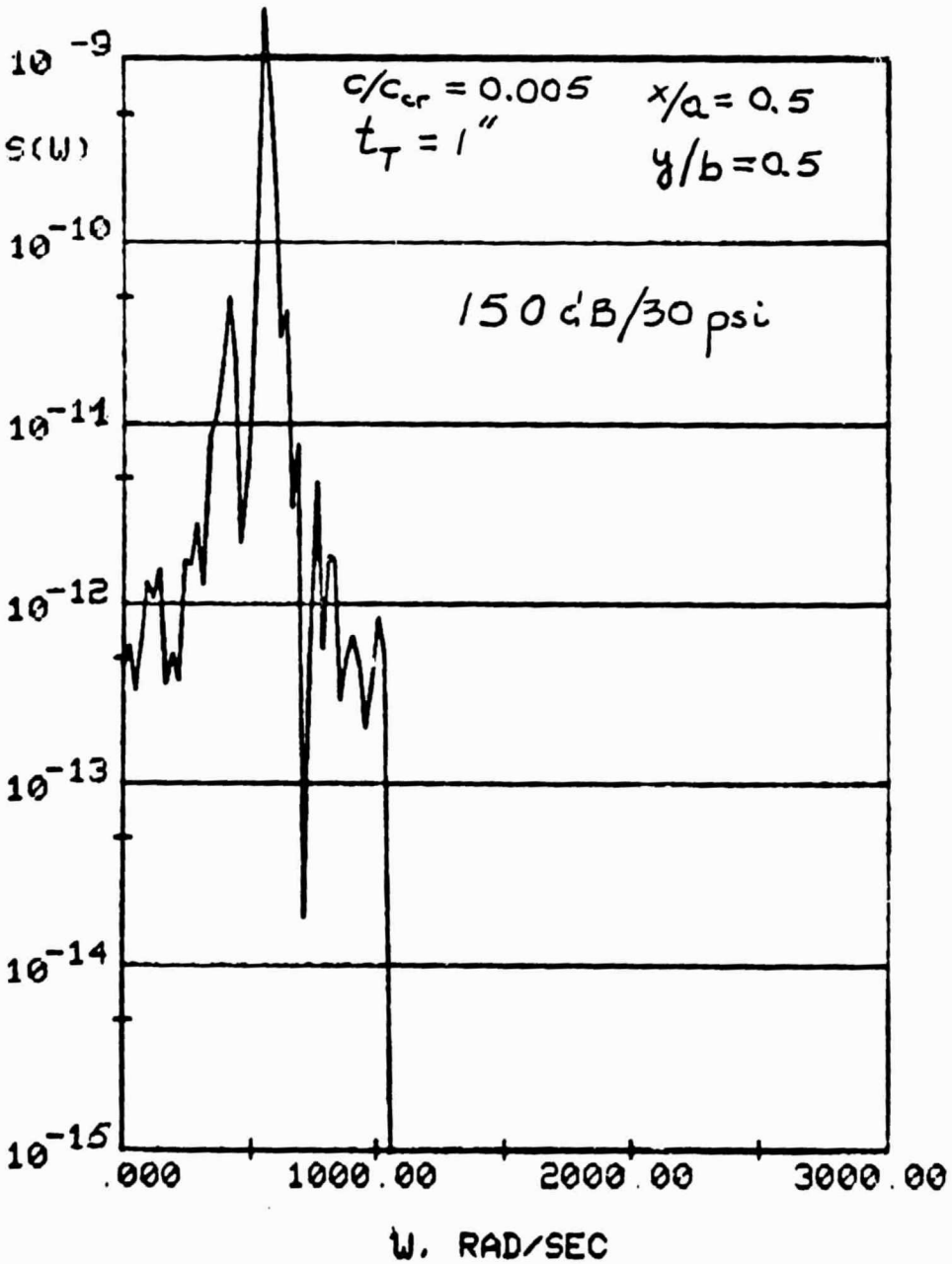

Fig. 11. Stringer Strain Spectral Density (c/c_{cr} = .005, t_T = 1")

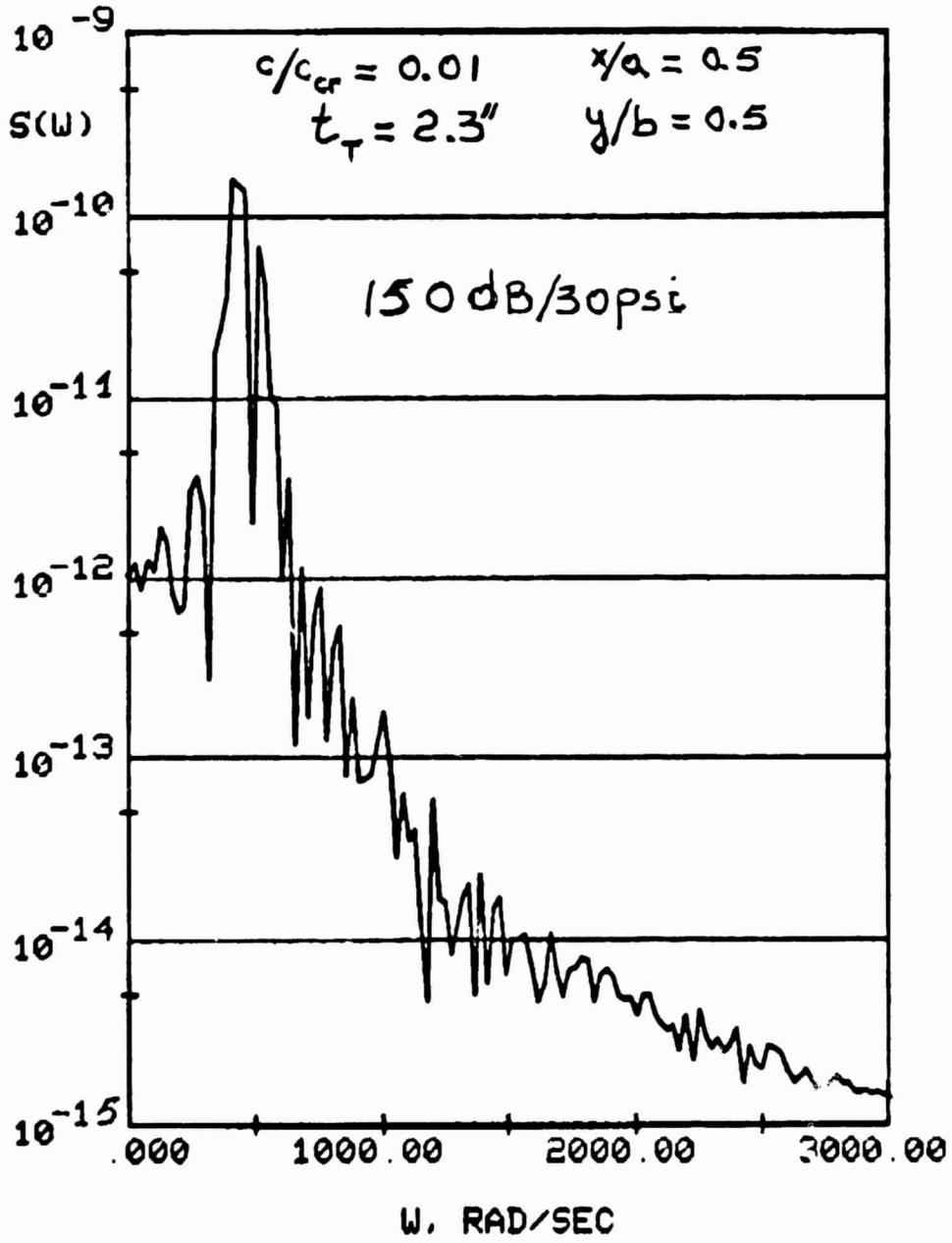

Fig. 12. Stringer Strain Spectral Density (c/c_{cr} = .01, t_T = 2.3")

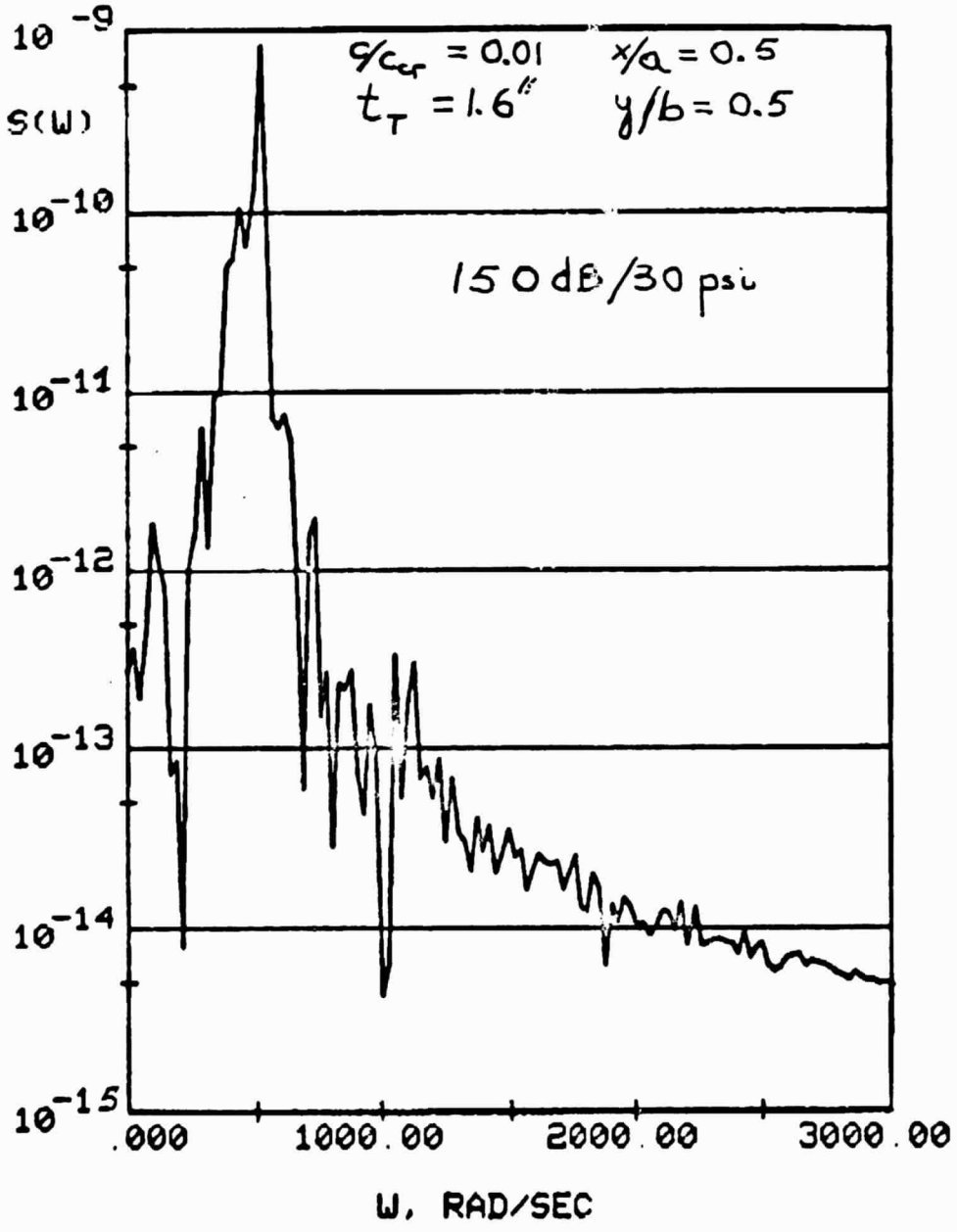

Fig. 13. Stringer Strain Spectral Density (c/c_{cr} = .01, t_T = 1.6")

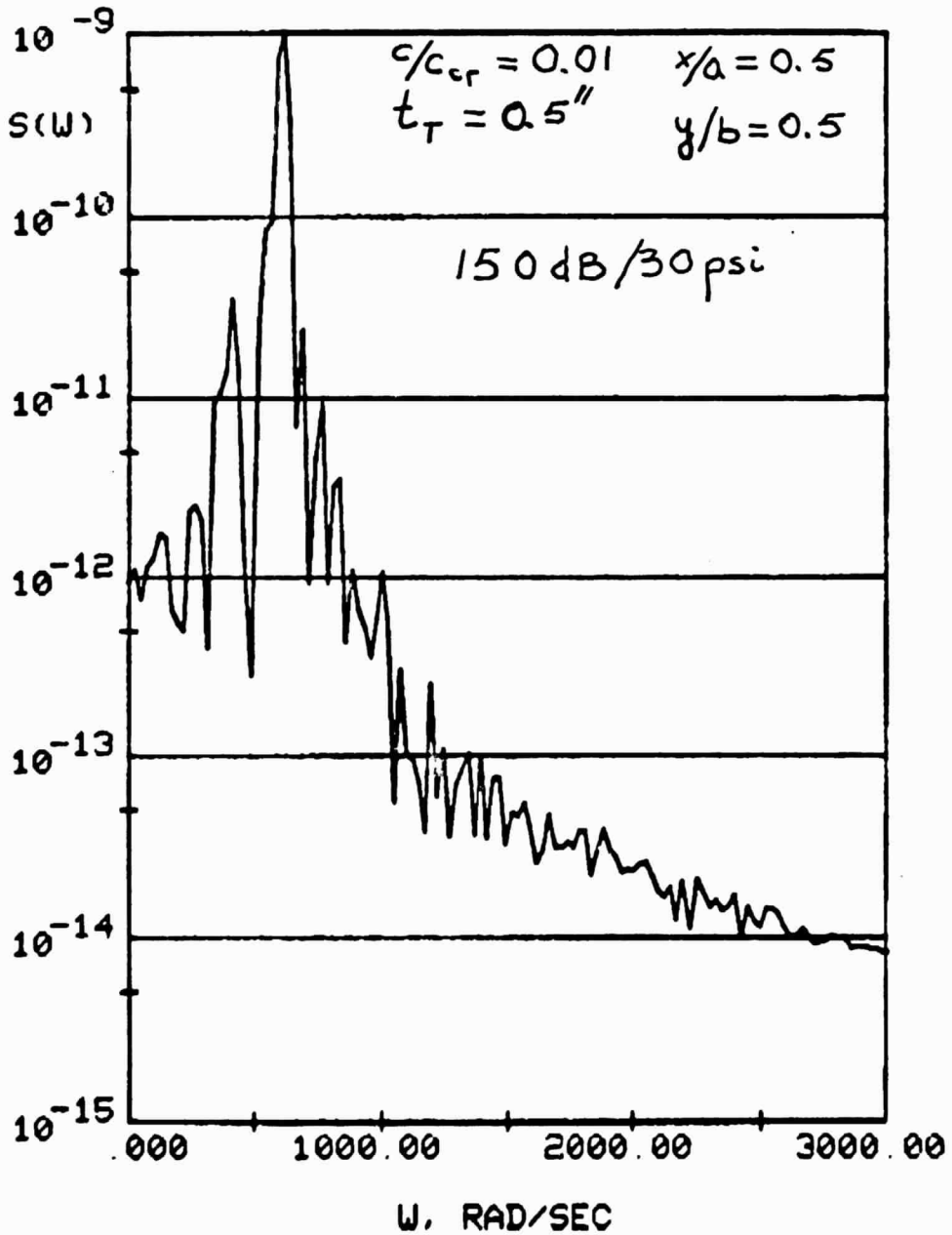

Fig. 14. Stringer Strain Spectral Density (c/c_{cr} = .01, t_T = .5")

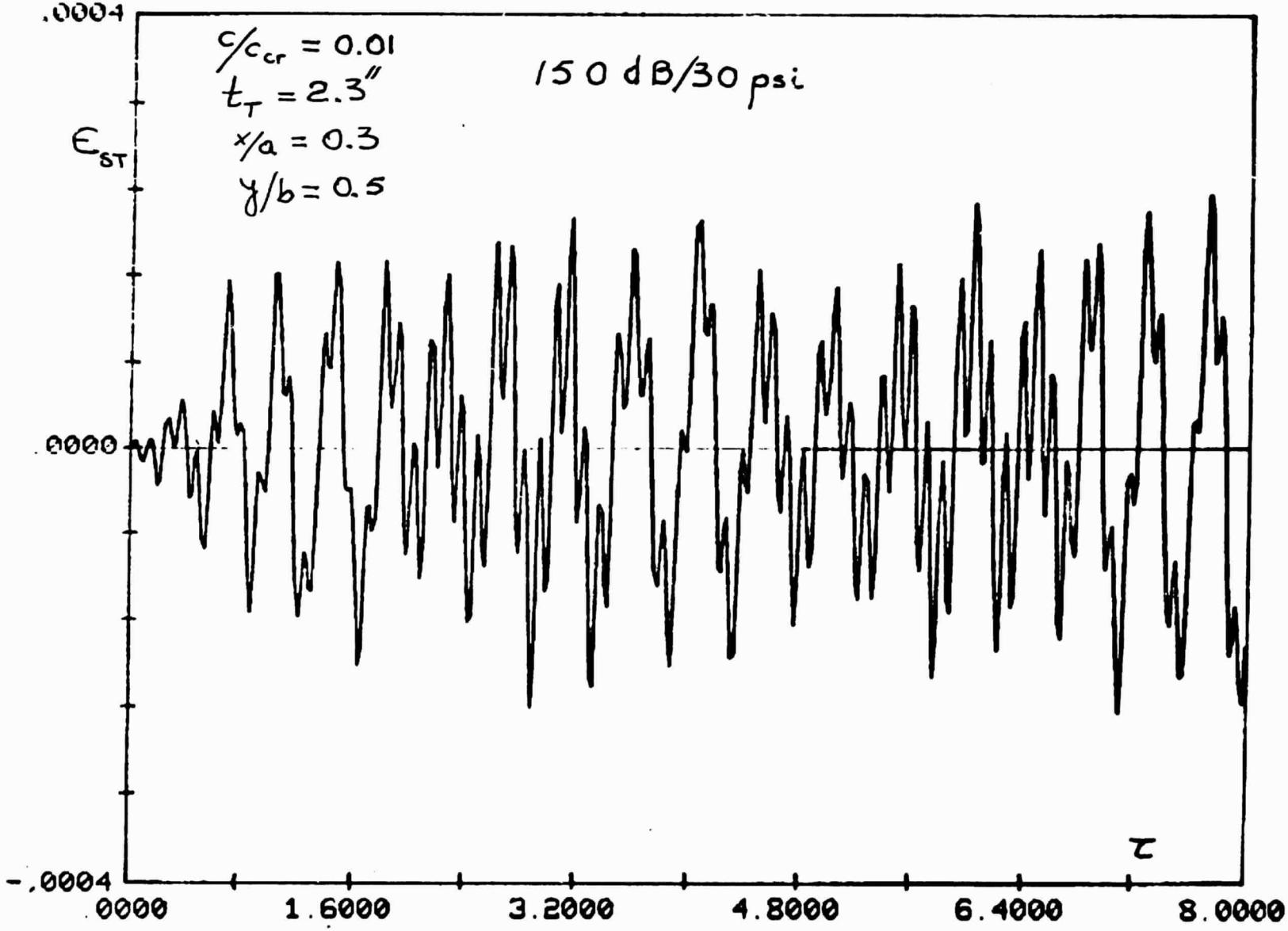

Fig. 15. Stringer Strain Time History at x/a = 0.3

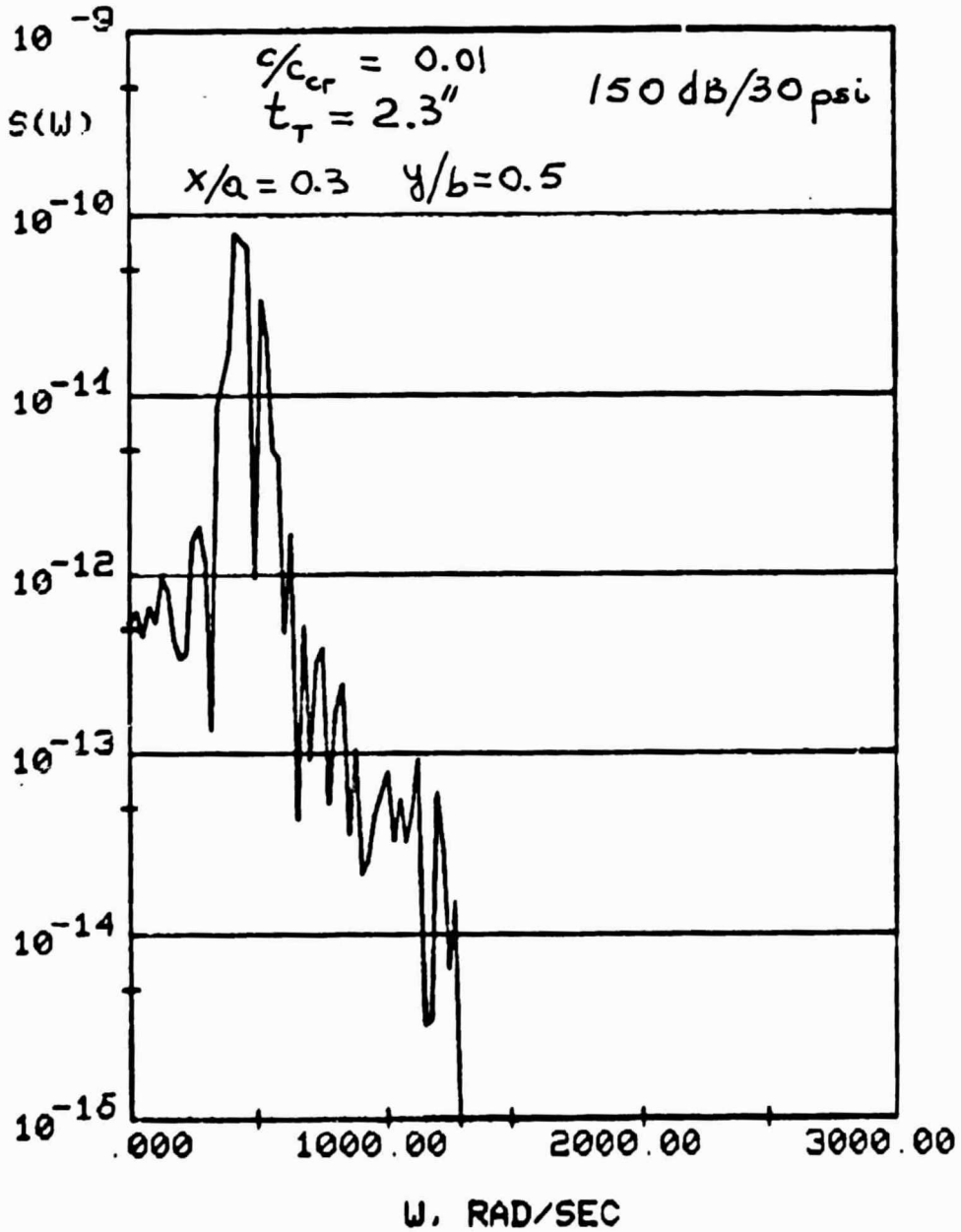

Fig. 16. Stringer Strain Spectral Density at x/a = 0.3